Preprints of the 21st IFAC World Congress (Virtual)
Berlin, Germany, July 12-17, 2020

Inter-Turn Short-Circuit Fault Ride-Through for DFIG Wind Turbines

Kuichao Ma * Jiangsheng Zhu *,** Mohsen Soltani *
Amin Hajizadeh * Zhe Chen ***

* Department of Energy Technology, Aalborg University, 6700 Esbjerg, Denmark (e-mail: kum,jzh,sms,aha@et.aau.dk)
** SEWPG European Innovation Center, Inge Lehmanns Gade 10, 8000 Aarhus, Denmark
*** Department of Energy Technology, Aalborg University, 9220 Aalborg, Denmark(e-mail: zch@et.aau.dk)

Abstract: Inter-Turn Short-Circuit (ITSC) of the stator winding is one of the most common faults in asynchronous generators. A significant feature of ITSC is the increase of the current in the faulty phase. Improper treatment may lead to unnecessary power loss or further deterioration. Therefore, this paper proposes a fault ride-through strategy under the stator ITSC fault for Doubly-Fed Induction Generator (DFIG) wind turbines. When the closed-loop state observer detects the fault and the current is higher than the rated current, the faulty wind turbine switches to down-regulation mode for protecting the faulty generator. The rotational speed reference is kept at the maximum value. Then the difference between the current and the rated current with the proportion-integration operation is superimposed to the original generator torque reference. Simulation results show that the faulty phase current can be decreased to the rated value, effectively. Although the power output is reduced as well, the impact of the fault does not develop to a failure. So the faulty wind turbine can continue to operate before the maintenance. The proposed strategy can avoid the unnecessary power loss caused by shut-down, improve the operational capacity of wind turbines and reduce the maintenance costs under the ITSC fault.

Keywords: Wind turbine, DFIG, Inter-turn short-circuit, Stator winding, Fault

1. INTRODUCTION

Wind power is one of the most widely used renewable energy sources. The development of related technologies is also rapid. At present, the capacity of the large offshore Wind Turbines (WTs) has reached 10 MW. The development of the offshore wind farm is quite rapid, especially in Europe. However, due to the harsh environment of the offshore wind farms, the high fault rate and the expensive maintenance costs constrain the development of the offshore wind energy Carroll et al. (2016).

Stator Inter-Turn Short-Circuit (ITSC) is one of the most common faults of induction machines Arkan et al. (2005). Many other failures can be seen as the result of a deterioration in ITSC fault Dybkowski and Bednarz (2019). That is because the ITSC fault can increase the faulty phase current and the temperature. ITSC fault has little impact at the early stage, but if not properly addressed, it will progress to some other faults, such as phase-phase or phase-ground short-circuit Tallam et al. (2000). In practice, there are two common ways to deal with the ITSC fault. One is to shut down the faulty WT for protection, and the other is to ignore the fault and continue to operate the faulty WT as normal. The power loss of the former is excessive, especially for large-capacity WTs. The latter may not have much impact on the WT at the beginning, but it will lead to other more serious faults or even failures. The main reason for the further deterioration of the fault is that the temperature of the faulty phase is very high when the WT is under high load condition. As a rule of thumb, the insulation lifetime is reduced by half for each 10 °C that the motor temperature exceeds its rated insulation temperature Venkataraman et al. (2005). Therefore, if the fault phase current does not exceed the rated current during operation, the generator can be protected from further damage due to the excessive temperature of the faulty winding.

Fault detection is the premise of the fault ride-through strategy. Many different approaches have been used for the fault detection of DFIGs Tchakoua et al. (2014). Motor Current Signature Analysis (MCSA) and wavelet analysis are widely used Douglas et al. (2005), Gritli et al. (2009). For wind power generation, the Luenberger observer method proposed in Lu et al. (2011) is more suitable. We adopt this method for stator ITSC fault detection. The main content of the fault ride-through strategy is to deal with the stator ITSC fault, effectively.

Different from the Fault Tolerant Control (FTC) strategy Sellami et al. (2017), the proposed strategy does not reduce the faulty phase current to the normal value by the complex current control but prevent the faulty phase from exceeding the rated current by the adjustment of the rotational speed and the power. This strategy can be implemented fast and feasible from practical point of view. However, the drawback is that the imbalance current is still exist. Therefore, the proposed strategy is more suitable for the early stage of the stator ITSC fault.

The contribution of this paper is that the excessive temperature caused by stator ITSC fault can be reduced by changing the rotational speed and the power. The strategy not only protects the faulty WT but also reduces the power loss as much as possible. Moreover, there is no need to calculate how much power should be down-regulated. The process of the fault level estimation is unnecessary as well.

The outline of this paper is given as follows. In Section 2, the state-space model of Doubly-Fed Induction Generator (DFIG) with stator ITSC fault in the stationary $\alpha\beta$ reference frame is presented. The normal control strategy is described in Section 3. Then, the fault ride-through strategy is proposed in Section 4. The simulation results are presented in Section 5. Finally, the conclusions are drawn in Section 6.

2. STATE-SPACE MODEL OF DFIG WITH ITSC FAULT IN STATOR

The mathematical models of DFIG in natural abc and stationary $\alpha\beta$ reference frames are well known in Abad et al. (2011). In order to design an observer for fault detection, the state-space model is necessary. By taking the currents and voltages as the state and input variables, the voltage and flux equations can be organized into a standard state-space form. In stationary $\alpha\beta$ reference frame, the state-space model of DFIG could be expressed by

$$\begin{cases} \dot{x} = Ax + Bu \\ y = Cx \end{cases}, \tag{1}$$

where the state variable vector, input variable vector and output variable vector, are $x = \left[i_{\mathrm{s}\alpha} \; i_{\mathrm{s}\beta} \; i_{\mathrm{r}\alpha} \; i_{\mathrm{r}\beta} \right]^{\mathrm{T}}$, $u = \left[v_{\mathrm{s}\alpha} \; v_{\mathrm{s}\beta} \; v_{\mathrm{r}\alpha} \; v_{\mathrm{r}\beta} \right]^{\mathrm{T}}$ and $y = \left[i_{\mathrm{s}\alpha} \; i_{\mathrm{s}\beta} \; i_{\mathrm{r}\alpha} \; i_{\mathrm{r}\beta} \right]^{\mathrm{T}}$, respectively. The subscripts s and r represent the stator and rotor. The state matrix A is given by

$$A = A_{\mathrm{c}} + A_{\mathrm{w}}\omega_{\mathrm{e}}, \tag{2}$$

where ω_{e} represents the electrical angular speed of the rotor, given by

$$\omega_{\mathrm{e}} = p\omega_{\mathrm{m}}, \tag{3}$$

where ω_{m} represents the mechanical angular speed of the rotor of the generator; p represents the number of pole-pairs.

The matrices A_{c} and A_{w} are as follows:

$$A_{\mathrm{c}} = \begin{bmatrix} -\dfrac{R_{\mathrm{s}}}{\sigma L_{\mathrm{s}}} & 0 & \dfrac{L_{\mathrm{m}}R_{\mathrm{r}}}{\sigma L_{\mathrm{s}}L_{\mathrm{r}}} & 0 \\ 0 & -\dfrac{R_{\mathrm{s}}}{\sigma L_{\mathrm{s}}} & 0 & \dfrac{L_{\mathrm{m}}R_{\mathrm{r}}}{\sigma L_{\mathrm{s}}L_{\mathrm{r}}} \\ \dfrac{L_{\mathrm{m}}R_{\mathrm{s}}}{\sigma L_{\mathrm{s}}L_{\mathrm{r}}} & 0 & -\dfrac{R_{\mathrm{r}}}{\sigma L_{\mathrm{r}}} & 0 \\ 0 & \dfrac{L_mR_{\mathrm{s}}}{\sigma L_{\mathrm{s}}L_{\mathrm{r}}} & 0 & -\dfrac{R_{\mathrm{r}}}{\sigma L_{\mathrm{r}}} \end{bmatrix}, \tag{4}$$

$$A_{\mathrm{w}} = \begin{bmatrix} 0 & \dfrac{1-\sigma}{\sigma} & 0 & \dfrac{L_{\mathrm{s}}}{\sigma L_{\mathrm{s}}} \\ -\dfrac{1-\sigma}{\sigma} & 0 & -\dfrac{L_{\mathrm{s}}}{\sigma L_{\mathrm{s}}} & 0 \\ 0 & -\dfrac{L_{\mathrm{s}}}{\sigma L_{\mathrm{r}}} & 0 & -\dfrac{1}{\sigma} \\ \dfrac{L_{\mathrm{s}}}{\sigma L_{\mathrm{r}}} & 0 & \dfrac{1}{\sigma} & 0 \end{bmatrix}, \tag{5}$$

where R_{s}, R_{r}, L_{s}, L_{r}, L_{m} and σ represent the stator resistance, rotor resistance, stator inductance, rotor inductance, mutual inductance and leakage coefficient, respectively. The leakage coefficient is given by

$$\sigma = \frac{L_{\mathrm{s}}L_{\mathrm{r}} - L_{\mathrm{m}}^2}{L_{\mathrm{s}}L_{\mathrm{r}}}. \tag{6}$$

The input matrix B is given by

$$B = \begin{bmatrix} \dfrac{1}{\sigma L_{\mathrm{s}}} & 0 & \dfrac{-L_{\mathrm{m}}}{\sigma L_{\mathrm{s}}L_{\mathrm{r}}} & 0 \\ 0 & \dfrac{1}{\sigma L_{\mathrm{s}}} & 0 & \dfrac{-L_{\mathrm{m}}}{\sigma L_{\mathrm{s}}L_{\mathrm{r}}} \\ \dfrac{-L_{\mathrm{m}}}{\sigma L_{\mathrm{s}}L_{\mathrm{r}}} & 0 & \dfrac{1}{\sigma L_{\mathrm{r}}} & 0 \\ 0 & \dfrac{-L_{\mathrm{m}}}{\sigma L_{\mathrm{s}}L_{\mathrm{r}}} & 0 & \dfrac{1}{\sigma L_{\mathrm{r}}} \end{bmatrix}. \tag{7}$$

The output matrix C is given by

$$C = \begin{bmatrix} 1 & 0 & 0 & 0 \\ 0 & 1 & 0 & 0 \\ 0 & 0 & 1 & 0 \\ 0 & 0 & 0 & 1 \end{bmatrix}. \tag{8}$$

The configuration of DFIG with stator ITSC fault in Phase A is shown in Fig. 1.

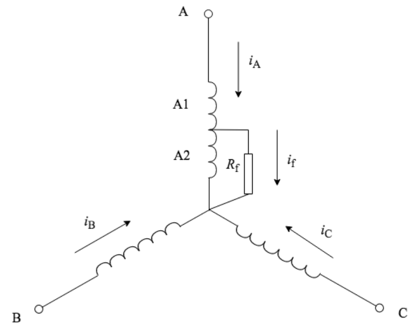

Fig. 1. Stator winding with ITSC fault in Phase A.

For describing the ITSC fault, two parameters μ and f_{x} are applied here to indicate the fault level and the fault position, respectively. μ is defined as the percentage of the number of the shorted turns to the number of the turns in the healthy phase. f_{x} represents the phase in which the fault occurred. In abc reference frame, The matrices of f_{x} corresponding to Phase A, B and C are as follows:

$$f_{\mathrm{A}} = \left[1 \;\; 0 \;\; 0 \right]^{\mathrm{T}}, f_{\mathrm{B}} = \left[0 \;\; 1 \;\; 0 \right]^{\mathrm{T}}, f_{\mathrm{C}} = \left[0 \;\; 0 \;\; 1 \right]^{\mathrm{T}}. \tag{9}$$

In stationary $\alpha\beta$ reference frame, f_{x} is converted as follows:

$$f_{\mathrm{A}} = \left[1 \;\; 0 \right]^{\mathrm{T}}, f_{\mathrm{B}} = \begin{bmatrix} -\dfrac{1}{2} & \dfrac{\sqrt{3}}{2} \end{bmatrix}^{\mathrm{T}}, f_{\mathrm{C}} = \begin{bmatrix} -\dfrac{1}{2} & -\dfrac{\sqrt{3}}{2} \end{bmatrix}^{\mathrm{T}}. \tag{10}$$

According to Lu et al. (2011), the state-space model of DFIG with ITSC fault in stator winding can be modified as

$$\dot{x} = Ax + Bu + \frac{1}{R_{\mathrm{s}}}\frac{2\mu}{2\mu - 3}A\begin{bmatrix} f_x f_x^{\mathrm{T}}\begin{bmatrix} v_{s\alpha} \\ v_{s\beta} \end{bmatrix} \\ 0 \\ 0 \end{bmatrix}. \tag{11}$$

3. NORMAL CONTROL STRATEGY OF WIND TURBINE

In general, the control system for variable speed WT has two degrees of freedom: generator torque and pitch angle. Fig. 2 shows the general control scheme.

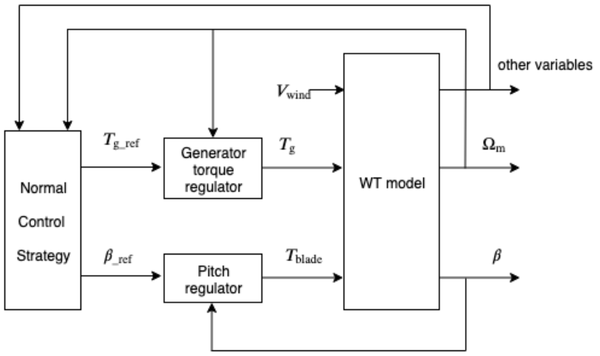

Fig. 2. Normal control strategy of WT.

Fig. 3 shows the most common speed curve of the WT. Four operation regions are divided according to the wind speed and the mechanical rotational speed Abad et al. (2011):

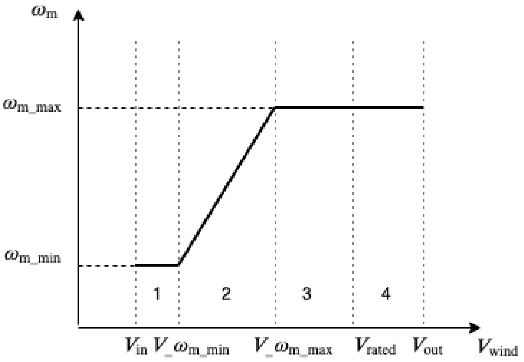

Fig. 3. Speed curve based on four speed regions.

1. Minimum speed operation region
2. Maximum Power Point Tracking (MPPT) region
3. Maximum speed in partial load region
4. Maximum speed in rated power region

In Region 1, the rotational speed is limited to the specified minimum rotational speed to prevent the tower from resonating due to the low rotational speed. Besides, the minimum rotational speed is also limited by the maximum power capacity of the rotor-side converter for DFIG.

In Region 2, pitch angle maintains at 0, MPPT strategy adjusts the Tip Speed Ratio (TSR) at the optimal value for maximizing the power output. This adjustment is through generator torque control. There are two common ways to realize MPPT. One is the Indirect Speed Controller (ISC), which set the generator torque reference according to the static state on the maximum power curve. The other is the Direct Speed Controller (DSC), which use the optimal rotational speed value as the reference of the rotational speed controller. The output of the controller is the generator torque reference.

In Region 3, the rotational speed is limited to the maximum value. Meanwhile, the power increases with the generator torque.

In Region 4, the rotational speed is also limited to the maximum value. Generator torque is set at the rated value. The pitch system adjusts the rotational speed. WT produces the rated power output.

The Normal control strategy can well meet the design requirements of the WT under the healthy condition. However, when the fault occurs, operating with the normal control strategy will increase the severity of the fault.

4. CONTROL STRATEGY FOR ITSC FAULT RIDE-THROUGH

Normally, there are two measures when a fault occurs on the WT. One is shutdown, and the other is to ignore the fault and continue to operate the faulty WT. For some low-severity faults, shutdown will result in unnecessary power loss. While ignoring the fault may lead to the further deterioration or even failure. Therefore, different measures should be taken for different fault scenarios.

4.1 Fault Analysis

The most significant effect of the ITSC fault is on the faulty phase current. The reduction of the effective impedance of the faulty phase will lead to the increase in the current Lu (2012). When the WT is operating under high load, the faulty phase current may exceed the rated current of the generator. Excessive current will cause the temperature of the winding to rise, and long-term operation in this condition can lead to further damage to the insulation layer. Therefore, the faulty phase current is the key to protecting the generator. Since the current of the generator is positively related to the power, the current can be reduced by down-regulating the WT. The faulty phase current will be reduced accordingly. As long as the current of the faulty phase does not exceed the rated current value, the generator fault will not be further aggravated. Moreover, excessive power loss can be avoided compared to shutting down the faulty WT directly.

Speed has a great effect on the power and the current for WT with DFIG. The effective value of the stator current can be expressed as

$$I_{\mathrm{s}} = \frac{P_{\mathrm{s}}}{\sqrt{3}U_{\mathrm{s}}\cos\phi} = \frac{P}{\sqrt{3}U_{\mathrm{s}}(1-s)\cos\phi}, \tag{12}$$

where P_{s}, U_{s}, P,ϕ and s represent the stator power, stator voltage, power output, phase angle and slip, respectively. Slip is defined as

$$s = \frac{\omega_{\mathrm{s}} - \omega_{\mathrm{e}}}{\omega_{\mathrm{s}}}, \tag{13}$$

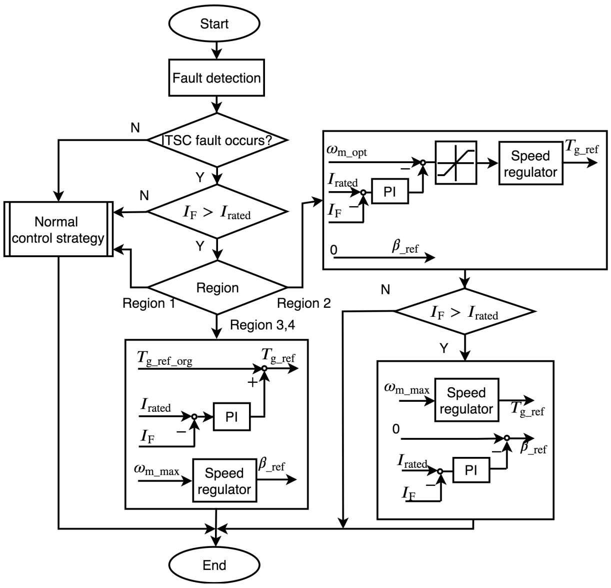

Fig. 4. Flowchart of fault ride-through strategy.

where ω_s represents the synchronous electrical angular speed.

When the rotational speed is higher than the synchronous rotational speed, the generator is in the super-synchronous state. s is a negative value. Both stator and rotor output the electrical power to the grid. According to (12) and (13), the higher the rotational speed, the lower the stator current. Therefore, when the ITSC fault in stator occurs, the rotational speed should be set as the maximum value. Otherwise, reducing the faulty phase current to the same value requires more power to be down-regulated.

4.2 Fault Detection

According to (11), the ITSC fault can be seen as an actuator fault. The commonly used closed-loop state observer (Luenberger observer) is used for detection Lu et al. (2011). Based on the state-space model of DFIG with stator ITSC fault , the observer can be constructed as

$$\begin{cases} \dot{\hat{x}} = A\hat{x} + Bu + K(y - C\hat{x}) \\ \hat{y} = C\hat{x} \end{cases}, \tag{14}$$

where estimated state vector, input variable vector and estimated output vector are defined as $\hat{x} = \begin{bmatrix} \hat{i_{s\alpha}} & \hat{i_{s\beta}} & \hat{i_{r\alpha}} & \hat{i_{r\beta}} \end{bmatrix}^T$, $u = \begin{bmatrix} v_{s\alpha} & v_{s\beta} & v_{r\alpha} & v_{r\beta} \end{bmatrix}^T$ and $\hat{y} = \begin{bmatrix} \hat{i_{s\alpha}} & \hat{i_{s\beta}} & \hat{i_{r\alpha}} & \hat{i_{r\beta}} \end{bmatrix}^T$.

Combining (11) and (14), the residual equation can be obtained as

$$\begin{aligned} \begin{bmatrix} \dot{e_{i_{s\alpha}}} \\ \dot{e_{i_{s\beta}}} \\ \dot{e_{i_{r\alpha}}} \\ \dot{e_{i_{r\beta}}} \end{bmatrix} &= (A - KC) \begin{bmatrix} e_{i_{s\alpha}} \\ e_{i_{s\beta}} \\ e_{i_{r\alpha}} \\ e_{i_{r\beta}} \end{bmatrix} \\ &\quad - \frac{1}{R_s} \frac{2\mu}{2\mu - 3} A \begin{bmatrix} f_x f_x^T \begin{bmatrix} v_{s\alpha} \\ v_{s\beta} \end{bmatrix} \\ 0 \\ 0 \end{bmatrix} \end{aligned} \tag{15}$$

Then, the fault can be detected by comparing the residual and the predefined threshold λ as follows

$$\begin{cases} \left\| \begin{bmatrix} e_{i_{s\alpha}} \\ e_{i_{s\beta}} \end{bmatrix} \right\|_\infty < \lambda; \text{ no fault occurs,} \\ \left\| \begin{bmatrix} e_{i_{s\alpha}} \\ e_{i_{s\beta}} \end{bmatrix} \right\|_\infty \geq \lambda; \text{ fault occurs.} \end{cases} \tag{16}$$

4.3 Fault Ride-Through Strategy

Fault ride-through strategy takes different approaches in different operation regions. The objective is that the faulty phase current does not exceed the rated current. The detail process and the activation conditions are shown in Fig. 4.

When the stator ITSC fault is detected, the faulty phase current and the rated current are compared. If the faulty phase current is lower than the rated current, the WT continues to operate according to the normal control strategy. Otherwise, the control strategy switches to the fault ride-through strategy.

For Region 1, the load of the generator is small, so even if the ITSC fault occurs, the faulty phase current will not exceed the rated current. WT operates as normal.

For Region 2, the pitch angle is 0 in normal condition, and the pitch system does not work except for providing aerodynamic brake. According to the above fault analysis, the stator current can be reduced by increasing the rotational speed. So DSC is used at first. Here, we perform the difference between the faulty phase current and the rated current with a Proportional Integral (PI) operation. The current difference term is used to adjust the reference. In this closed-loop, the faulty phase current can be seen as feedback. The upper limit of the rotational speed reference is the maximum rotational speed value. The difference between original rotational speed reference and the current difference term is set as the reference of DSC.

If the rotational speed has reached the maximum value and the faulty phase current is still higher than the rated current, the pitch control is activated to further down-regulate the WT. Similar to the adjustment of the generator torque reference, the difference between the original pitch angle reference (0 degrees) and the current difference term is set as the reference of the pitch system. However, the load of the WT in Region 2 is still small. The faulty phase current is rarely higher than the rated current unless the fault level is very high.

For Region 3 and 4, the rotational speed is already at the maximum value. The adjustment of the rotational speed is through the pitch control. So the main action in this situation is the setting of the generator torque reference. Firstly, the rotational speed must maintain at the maximum value, even if the WT is in down-regulation mode due to the power reference from the wind farm controller. Then, the WT is down-regulated by the adjustment of the generator torque reference. For reducing the faulty phase current, the current difference term is added to the original generator torque reference, which is calculated by the ratio of the power reference to the rotational speed.

It should be noted that there is a lower limit for the down-regulation rate. Typically, the rate should not be higher than 40% Knudsen et al. (2015).

5. SIMULATION RESULTS

The simulation is based on the modified NREL 5MW WT. The parameters of the WT and DFIG are extracted from SimWindFarm toolbox Grunnet et al. (2010) and Lei (2014), respectively. Since the stator current is greater under high load, we simulated the WT in Region 4 to verify the effectiveness of the proposed strategy. The wind speed is 12 m/s. A 5% ITSC fault occurs in Phase A at t = 30s. Fig. 5 shows the transient behaviour of the stator currents. It can be seen that, when the fault occurred, the amplitude of the faulty phase current increased. The current of the healthy phase did not change. The stator currents became unbalanced.

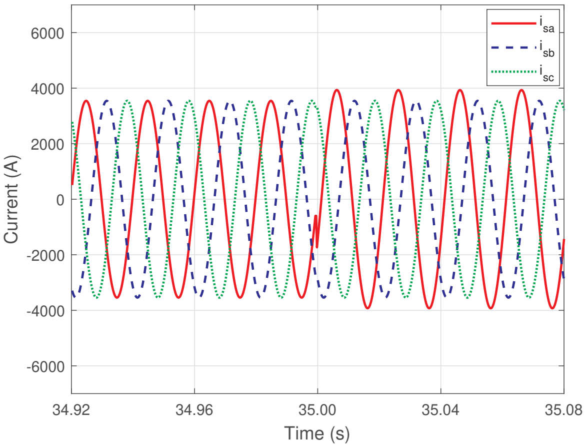

Fig. 5. transient stator current under ITSC, $\mu = 5\%$.

The simulation of fault detection is shown in Fig. 6. When the fault occurred, the residual of $i_{s\alpha}$ changed significantly. So the fault detection based on the Luenberger observer is effective for the ITSC fault.

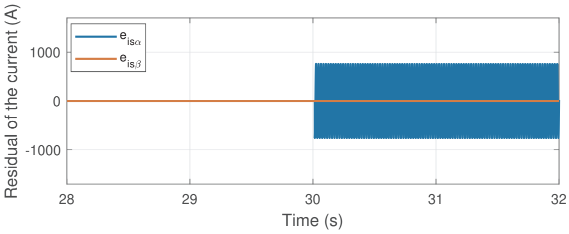

Fig. 6. Residuals of stator current in stationary $\alpha\beta$ reference frame.

When the fault is detected and the faulty phase current is higher than the rated current 2507 A, the control strategy will be switched from normal to fault ride-through mode. In order to show the effect of the proposed strategy clearly, fault ride-through strategy was activated at t=35s. The results are shown in Fig. 7 - Fig.12. The changes before and after t=35s are very obvious.

In Fig. 7, the rotational speed reference maintains at 1173.7 r/min. The fluctuation after t=35s is due to the sudden drop of the torque and the slow execution of the pitch system. Since the adjustment of the torque is much faster comparing with the pitch angle, the change rate of the torque should be limited to avoid the rotational speed fluctuation.

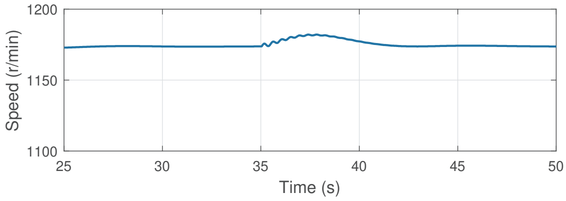

Fig. 7. Generator rotational speed under fault ride-through strategy.

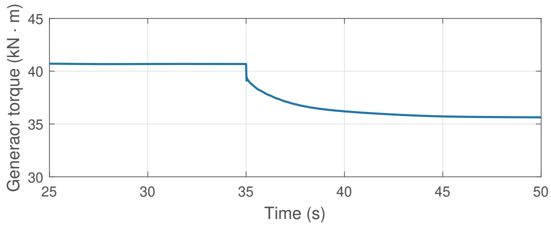

Fig. 8. Generaor torque under fault ride-through strategy.

As the strategy was activated, the generator torque was decreased from 43.4 to 35.6 kN · m to down-regulate the WT.

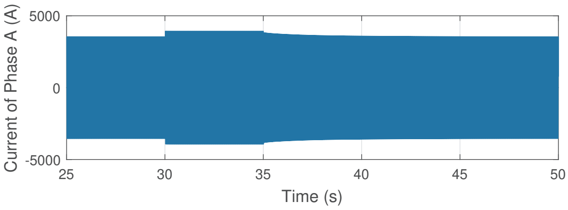

Fig. 9. Current of the faulty phase.

Fig. 9 shows the change of the current in the faulty phase. The current increased as the fault occurred. When the fault ride-through strategy started, the current decreased to the rated value. The effective current in Fig. 10 obviously shows the effect of the proposed strategy.

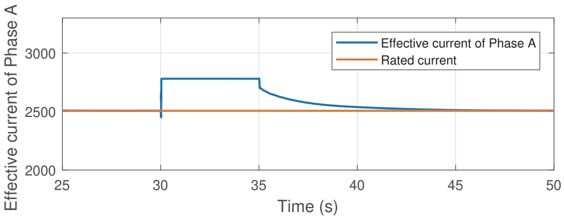

Fig. 10. Effective current of the faulty phase under fault ride-through strategy.

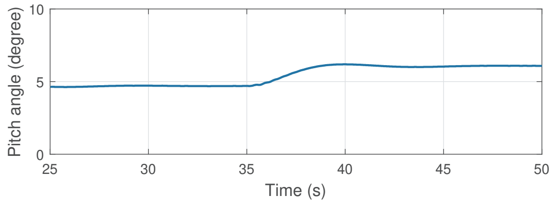

Fig. 11. Pitch angle under fault ride-through strategy.

Fig. 11 shows the pitch angle of the WT. Before the change of strategy, the value is around 4.7 degrees. To maintain the rotational speed constant, when the generator torque decreased, the pitch angle increased to 6.1 degrees to decrease the coefficient of the power. Then, the aerodynamic torque can match the change of the generator torque.

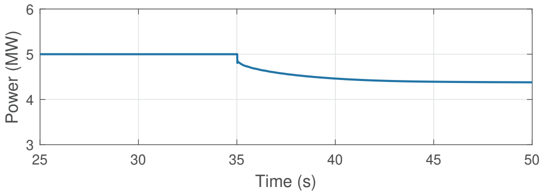

Fig. 12. Power under fault ride-through strategy.

Since the rotational speed was kept at the maximum value and the generator torque was reduced. The power of the WT decreased from 5 to 4.38 MW. Although the power of the WT is reduced, it is still much better than shut-down.

6. CONCLUSIONS

In this paper, we proposed a fault ride-through strategy for stator ITSC fault of DFIG wind turbine.

This strategy allows the WT to reduce part of the power to continue operation while protecting the faulty generator under high load conditions. The unnecessary power loss caused by shut-down can be avoided. The ability of the WT for operating under fault condition has been improved. The strategy is more effective for the offshore WTs with a high fault rate and expensive maintenance costs.

In future work, this strategy will be combined with the wind farm control to reduce the effect of the faulty WT on the performance of the wind farm. The other generator fault with similar characteristics to the stator ITSC fault will be studied to expand the application of the proposed strategy.

REFERENCES

Abad, G., Lopez, J., Rodriguez, M., Marroyo, L., and Iwanski, G. (2011). *Doubly fed induction machine: modeling and control for wind energy generation*, volume 85. John Wiley & Sons.

Arkan, M., Kostic-Perovic, D., and Unsworth, P. (2005). Modelling and simulation of induction motors with inter-turn faults for diagnostics. *Electric Power Systems Research*, 75(1), 57–66.

Carroll, J., McDonald, A., and McMillan, D. (2016). Failure rate, repair time and unscheduled o&m cost analysis of offshore wind turbines. *Wind Energy*, 19(6), 1107–1119.

Douglas, H., Pillay, P., and Barendse, P. (2005). The detection of interturn stator faults in doubly-fed induction generators. In *Fourtieth IAS Annual Meeting. Conference Record of the 2005 Industry Applications Conference, 2005.*, volume 2, 1097–1102. IEEE.

Dybkowski, M. and Bednarz, S.A. (2019). Modified rotor flux estimators for stator-fault-tolerant vector controlled induction motor drives. *Energies*, 12(17), 3232.

Gritli, Y., Stefani, A., Filippetti, F., and Chatti, A. (2009). Stator fault analysis based on wavelet technique for wind turbines equipped with dfig. In *2009 International Conference on Clean Electrical Power*, 485–491. IEEE.

Grunnet, J.D., Soltani, M., Knudsen, T., Kragelund, M., and Bak, T. (2010). Aeolus toolbox for dynamics wind farm model, simulation and control. In *European Wind Energy Conference and Exhibition, The European Academy of Wind Energy, EWEC*, 3119–3129.

Knudsen, T., Bak, T., and Svenstrup, M. (2015). Survey of wind farm control—power and fatigue optimization. *Wind Energy*, 18(8), 1333–1351.

Lei, T. (2014). *Doubly-fed induction generator wind turbine modelling, control and reliability*. Ph.D. thesis, The University of Manchester (United Kingdom).

Lu, Q. (2012). *Fault Diagnosis and Fault Tolerant Control of DFIG Based Wind Turbine System*. Ph.D. thesis, University of Manchester.

Lu, Q., Breikin, T., and Wang, H. (2011). Modelling and fault diagnosis of stator inter-turn short circuit in doubly fed induction generators. *IFAC Proceedings Volumes*, 44(1), 1013–1018.

Sellami, T., Berriri, H., Jelassi, S., Darcherif, A.M., and Mimouni, M.F. (2017). Short-circuit fault tolerant control of a wind turbine driven induction generator based on sliding mode observers. *Energies*, 10(10), 1611.

Tallam, R.M., Habetler, T.G., and Harley, R.G. (2000). Transient model for induction machines with stator winding turn faults. *Conference Record of the 2000 IEEE Industry Applications Conference. Thirty-Fifth IAS Annual Meeting and World Conference on Industrial Applications of Electrical Energy (Cat. No.00CH37129)*, 1, 304–309 vol.1.

Tchakoua, P., Wamkeue, R., Ouhrouche, M., Slaoui-Hasnaoui, F., Tameghe, T.A., and Ekemb, G. (2014). Wind turbine condition monitoring: State-of-the-art review, new trends, and future challenges. *Energies*, 7(4), 2595–2630.

Venkataraman, B., Godsey, B., Premerlani, W., Shulman, E., Thaku, M., and Midence, R. (2005). Fundamentals of a motor thermal model and its applications in motor protection. In *58th Annual Conference for Protective Relay Engineers, 2005.*, 127–144. IEEE.